

Spectral X-rays study of Seyfert 1 AGNs

Mónica Cardaci



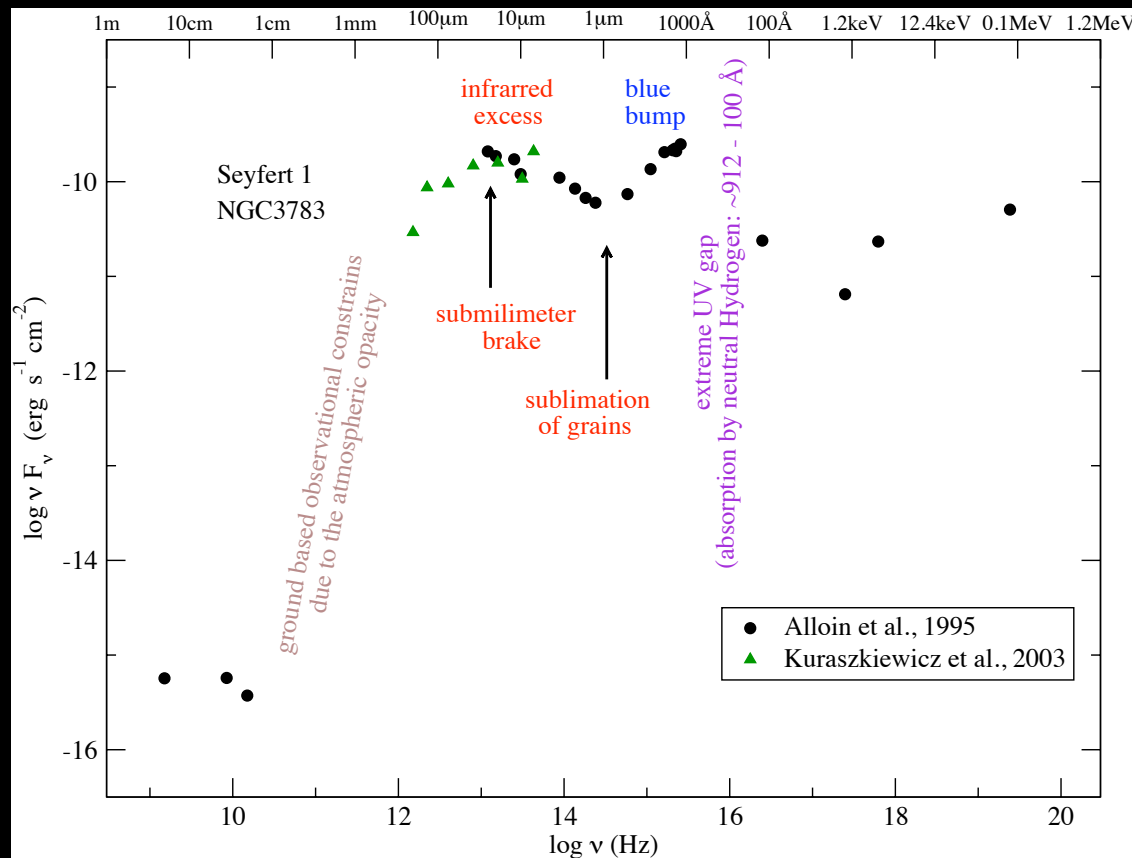
Intro

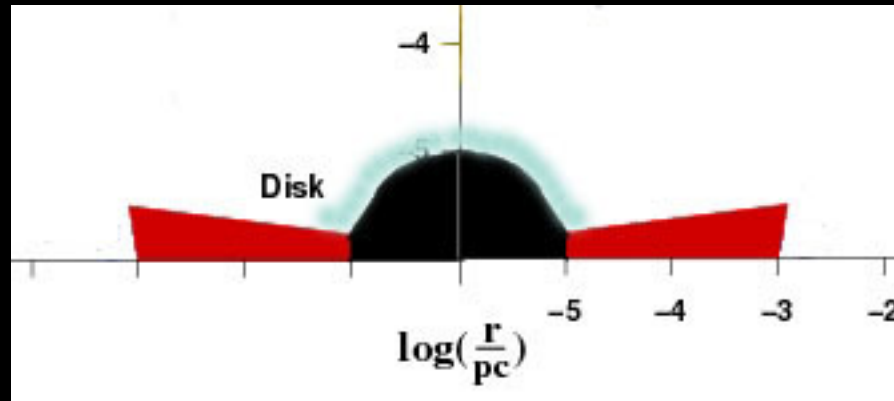
The AGNs are among the most **luminous** objects in the sky ($\sim 10^{42} - 10^{48}$ erg/s) in small volumes ($\ll 1$ pc³)

Most AGNs have some type of **variability** in time scales from days to years.

Intro

The radiation is emitted over a **wide spectral range** of frequencies from radio to gamma-rays, showing a roughly **flat spectral energy distribution** (SED) from the mid-infrared to hard X-rays .

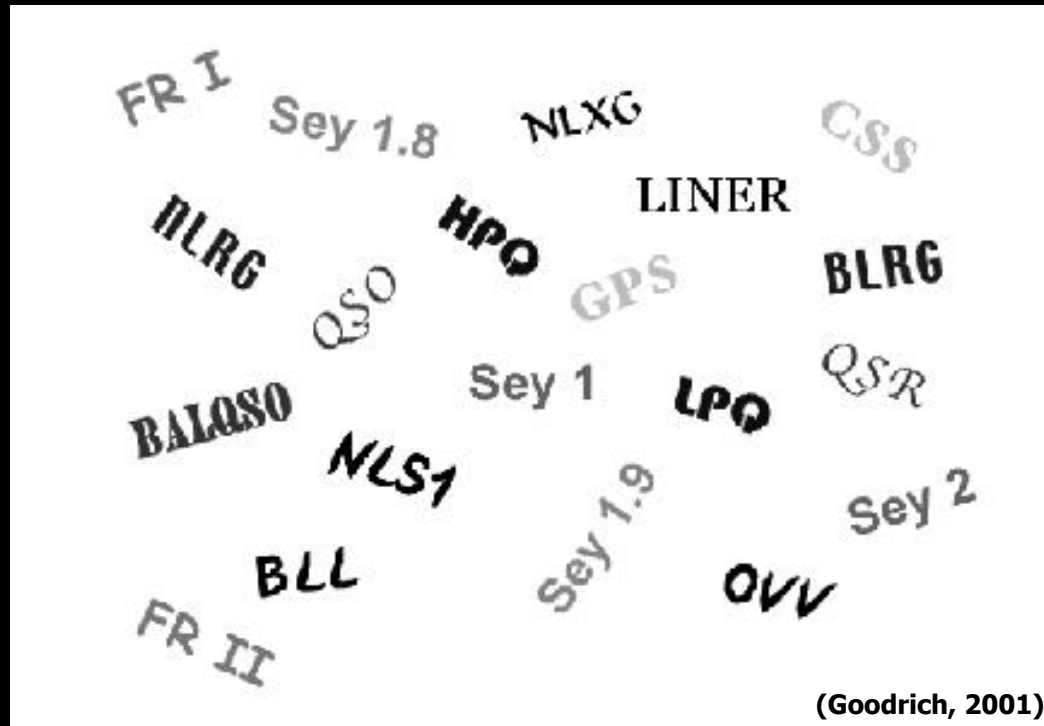


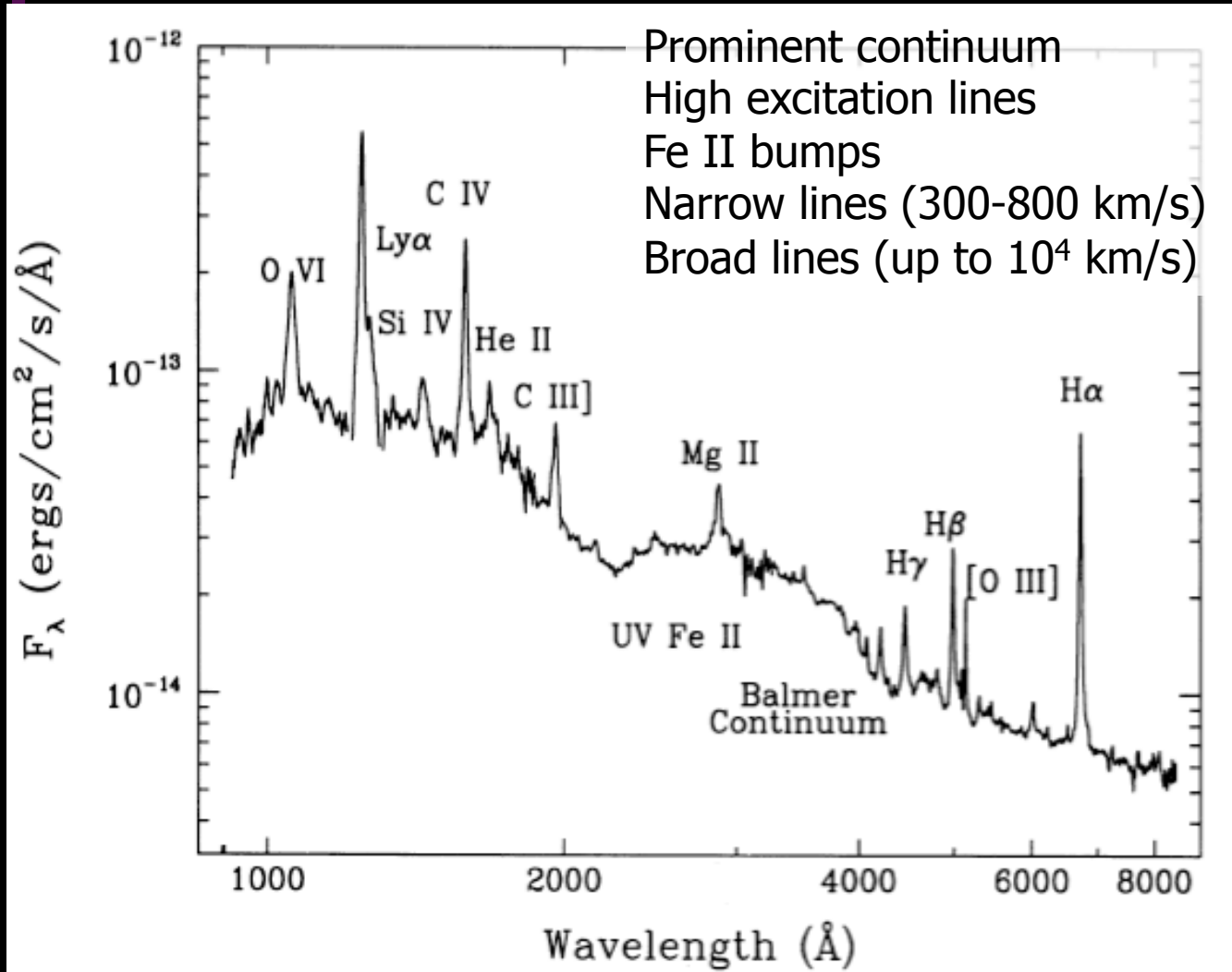


X-rays are produced in the innermost zone of the AGN.
About the 10% of the bolometric luminosity is emitted in X-rays

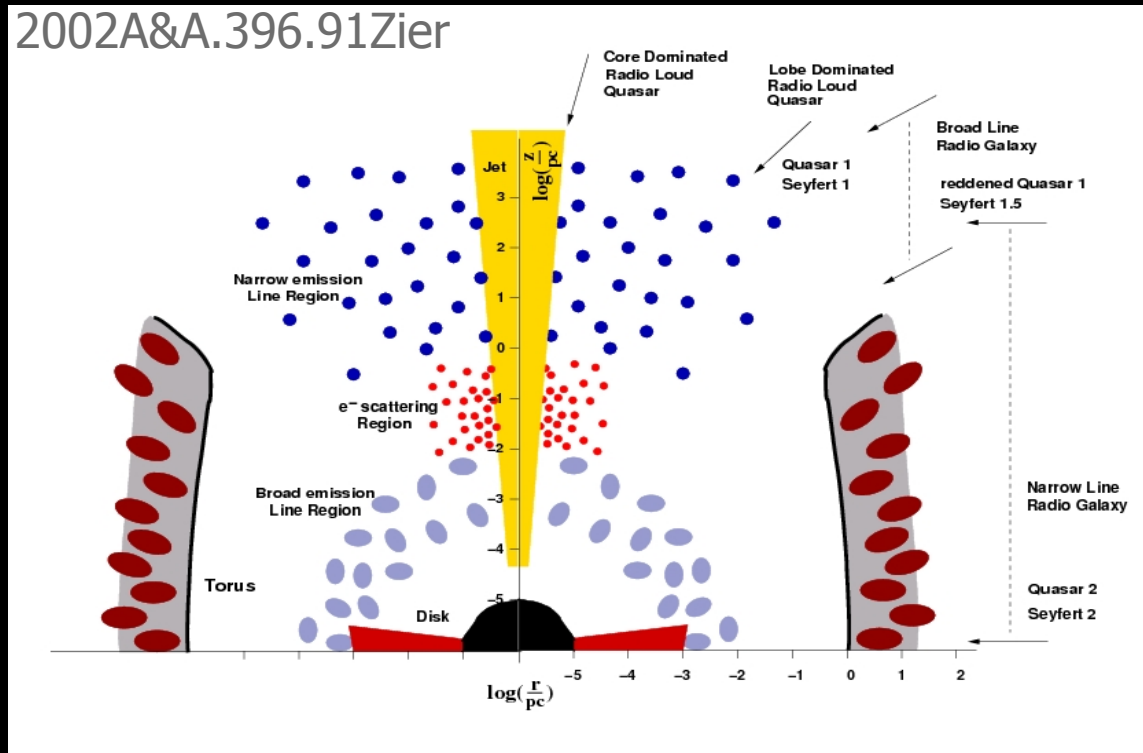
Intro

Depending on some relevant feature in the bandwidth used at the moment of the identification the AGNs have been classified in different ways





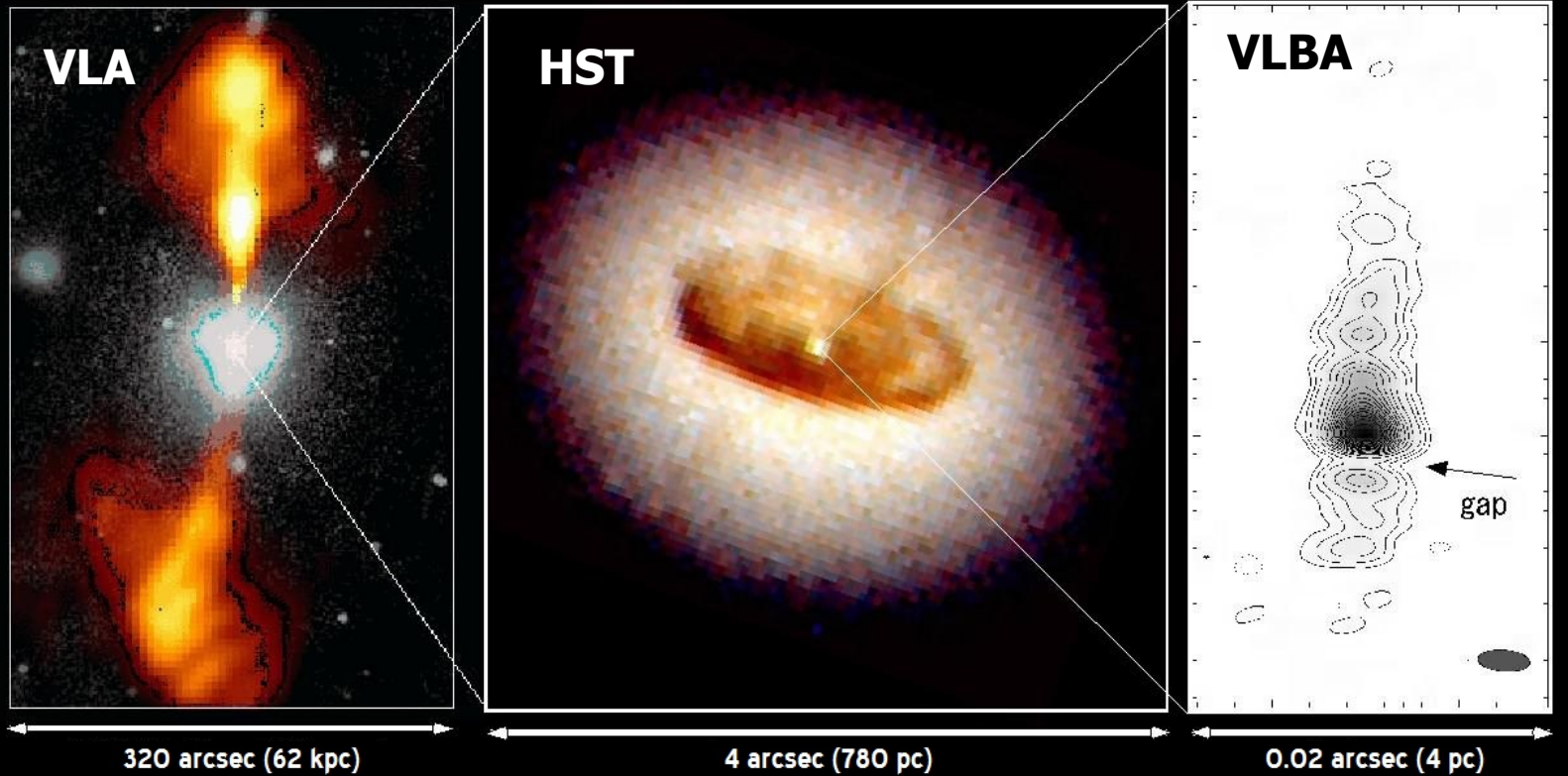
AGN ingredients



BH ($10^6 - 10^9 M_{\odot}$) – accretion disc – Broad Line region – dense torous – Narrow Line region – (energetic jet)

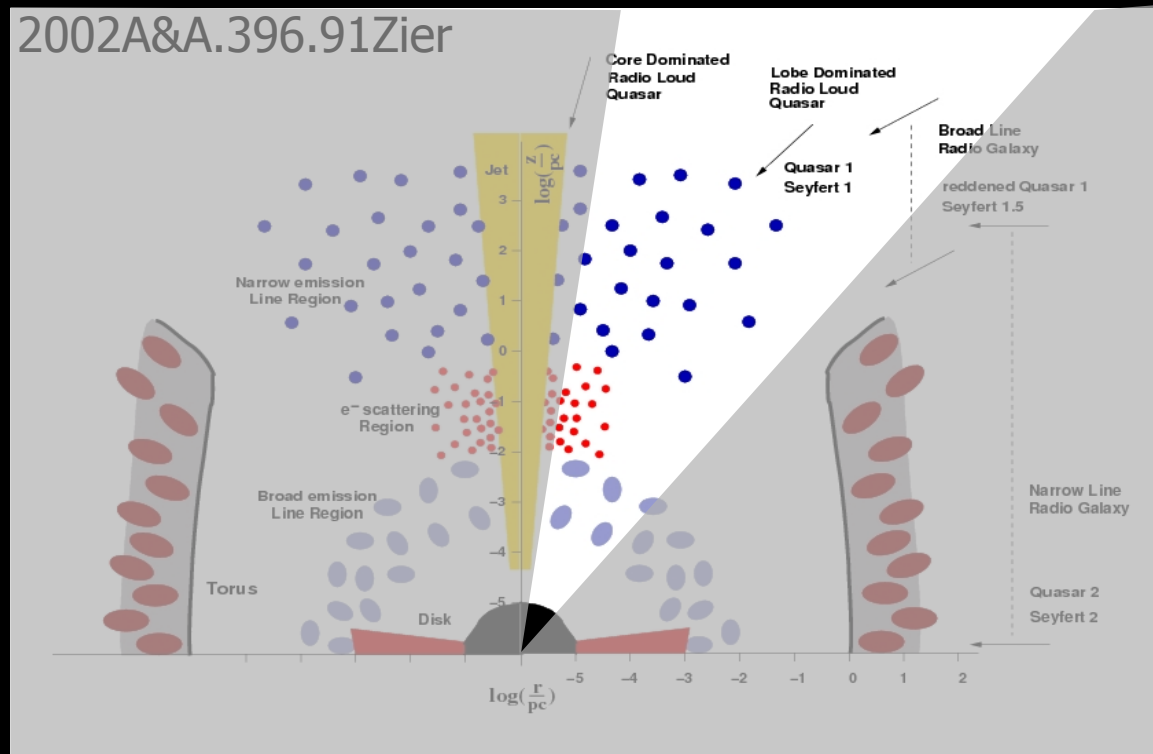
AGN ingredients

NGC 4261



Taken from the web site of Iguchi, S (2010)

Seyfert 1 zone (unified model)



$10^6 - 10^9 M_{\odot}$

$\sim 10^{11} L_{\odot}$

Intro

The immediate aim of this work is to characterize the **physical conditions** of the material in which the emission and absorption features are produced.

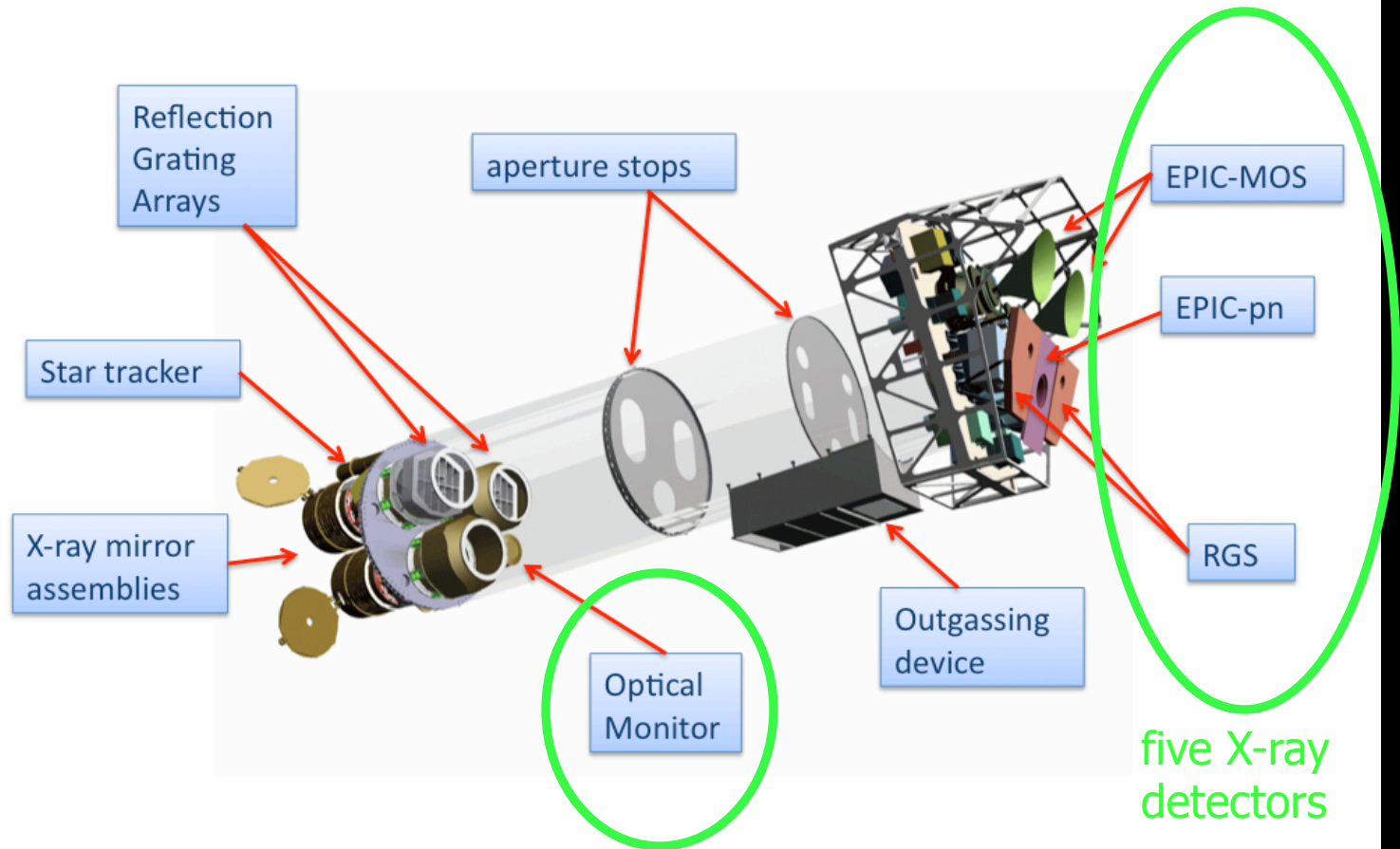
The more ambitious aim is to provide a general description of the typical physical conditions of the material associated to the AGN systems.

The objects analysed in this first work were 5 **bright Seyfert 1s** located at galactic coordinates where the H column densities are low ($N_{\text{H}} \sim 10^{20} \text{ cm}^{-2}$) to favor soft X-rays studies.

They were observed with **exposure times** longer than the average to favour the analysis of the High-resolution soft X-rays data.

XMM-Newton satellite

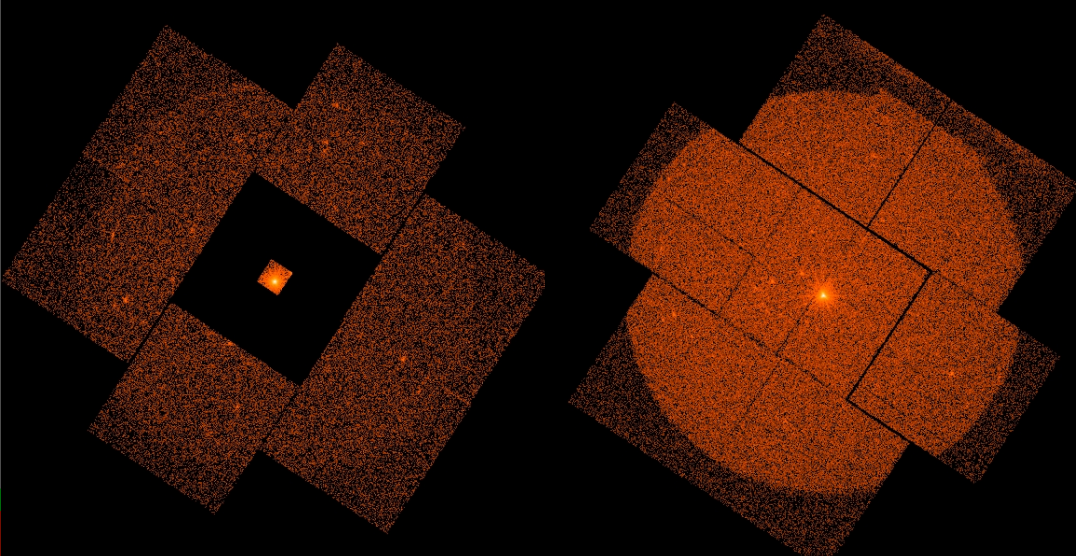
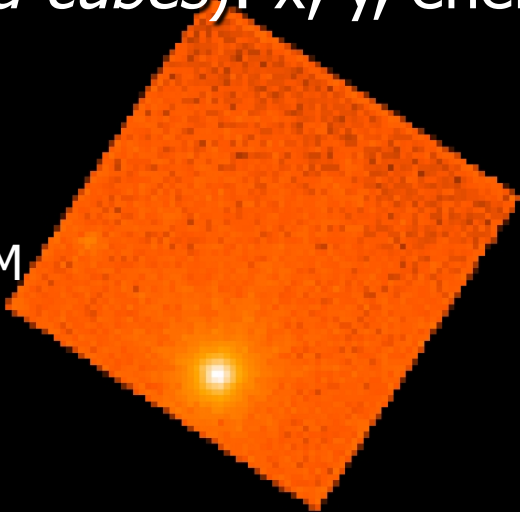
We analyzed data acquired with the XMM-Newton satellite of 5 selected AGNs



Data from the XMM-Newton

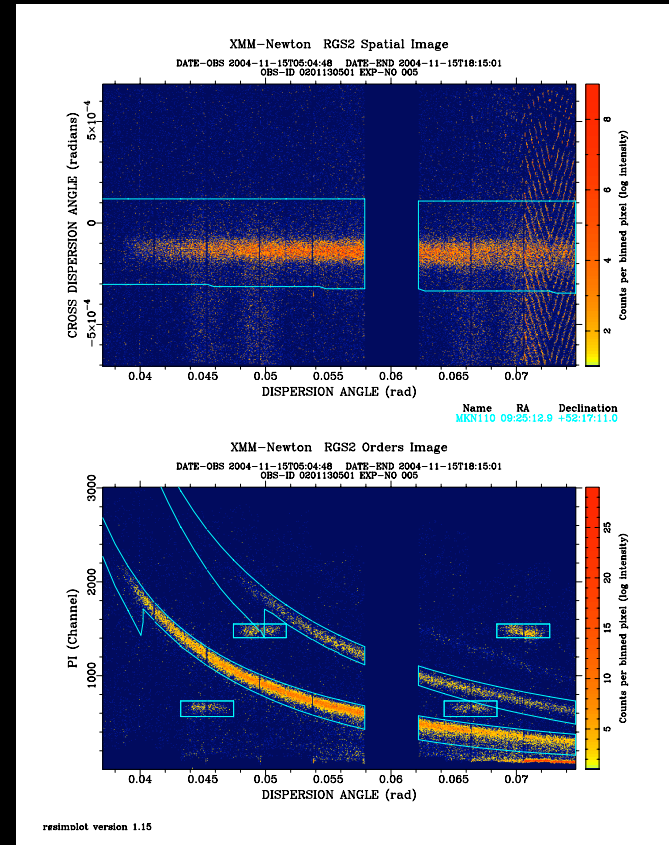
EPIC cameras: four dimensional data cubes (*tetra-cubes*): x , y , energy, time

0.1 – 15 keV
($\sim 0.8 - 120 \text{ \AA}$)
 $E/\Delta E \sim 20-50$
PSF: $\sim 6''$ FWHM



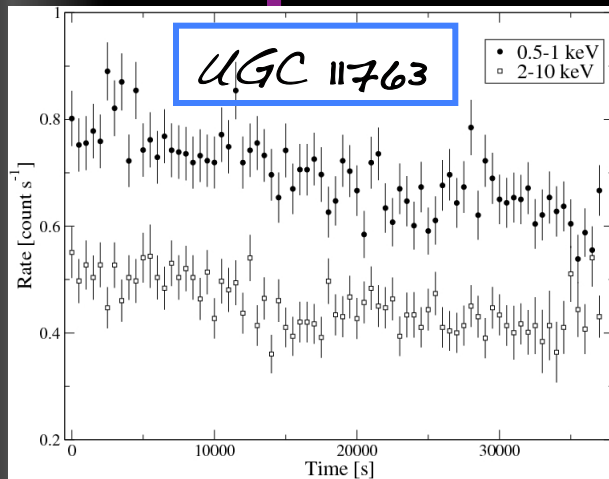
RGS spectrographs: wavelength & time

5 – 35 \AA
 $\lambda/\Delta\lambda \sim 150-800$

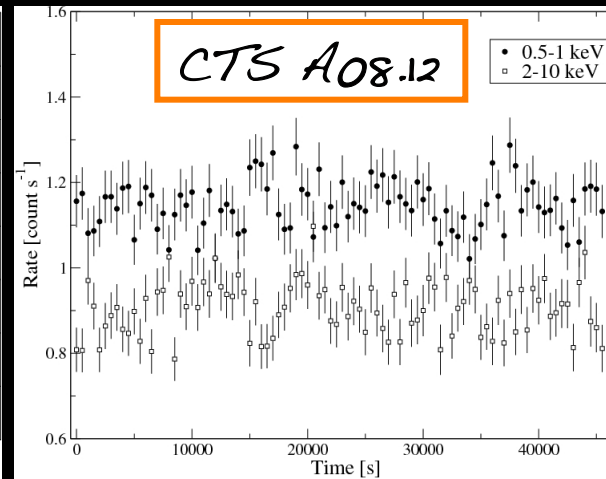


X-ray light curves

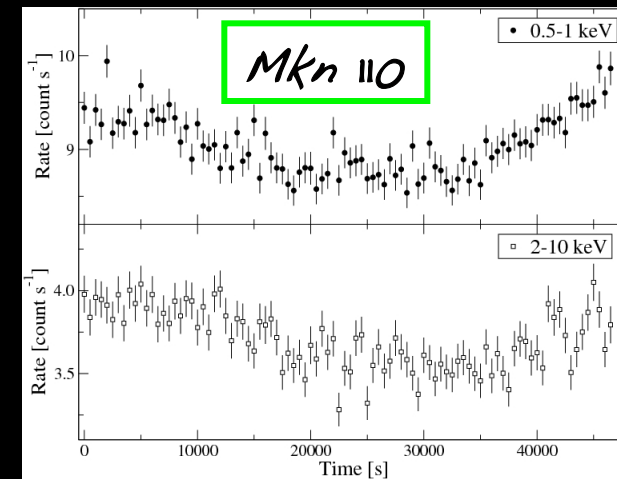
Time variability: Soft and hard X-ray light curves



(Cardaci et al. 2009).
**joint linear decrement
during the observation**



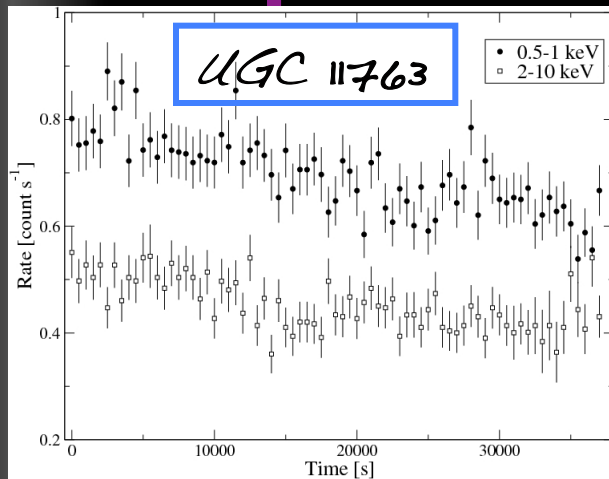
(Cardaci et al. 2011).
anti-correlation!!!!!!!



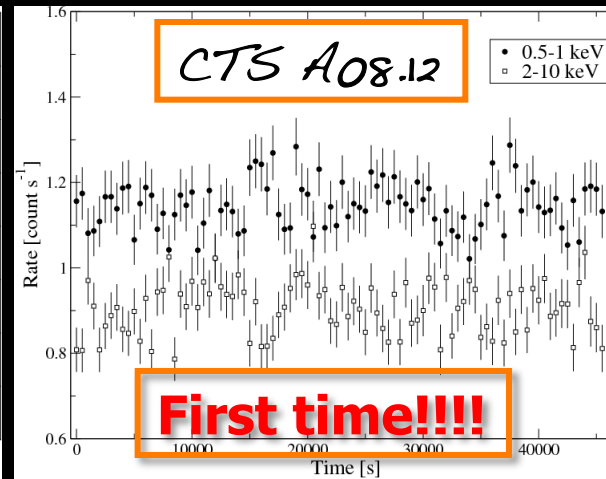
(Cardaci et al. 2011).
**a 1000s (~17m) delay is
observed, flux
variations in the hard
band come after the
ones in the soft band**

X-ray light curves

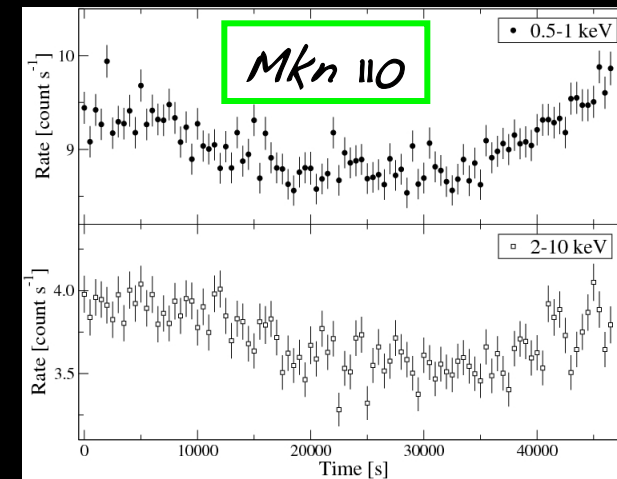
Time variability: Soft and hard X-ray light curves



(Cardaci et al. 2009).
**joint linear decrement
during the observation**



(Cardaci et al. 2011).
anti-correlation!!!!!!!!!!



(Cardaci et al. 2011).
**a 1000s (~17m) delay is
observed, flux
variations in the hard
band come after the
ones in the soft band**

X-ray spectral analysis

Comprehensive method

continuum:

- ✓ EPIC-pn spectrum to obtain a 1st approach to the hard band (2-10 keV) continuum

EPIC-pn whole range (0.35-2 keV) to check the 1st general hard continuum shape on the soft band

- ✓ EPIC-MOS and EPIC-pn spectra (all together) to provide a good continuum 0.35-10 keV description

all features:

- ✓ simultaneous EPIC & RGS fit (0.35-10 & 0.41-1.8 keV ranges)

X-ray spectral analysis

The model components

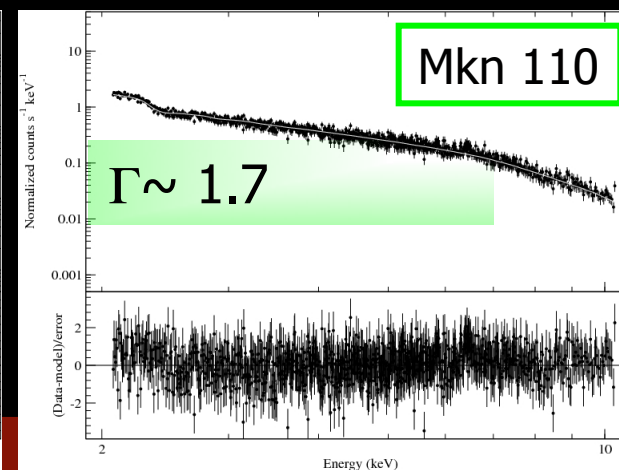
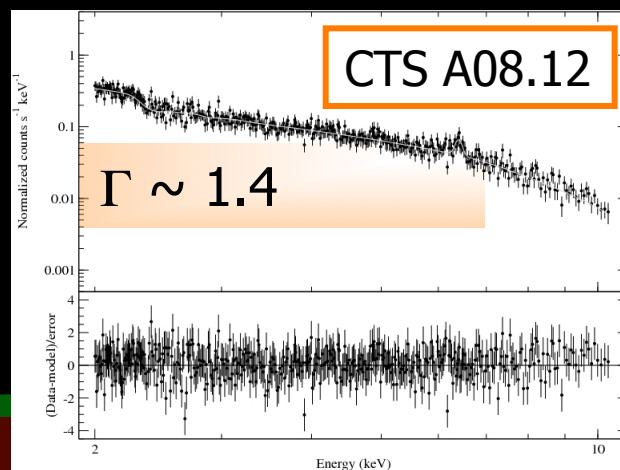
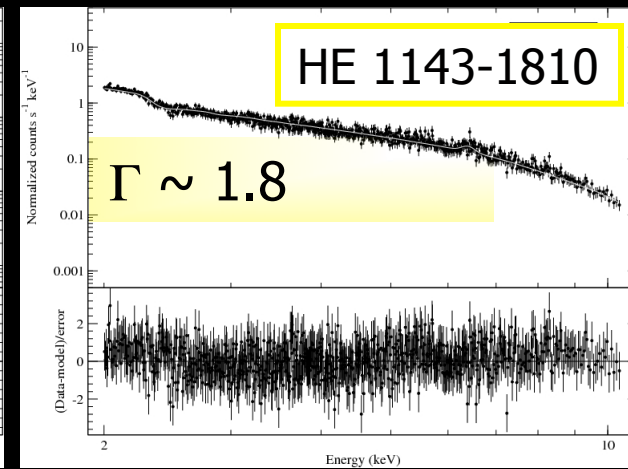
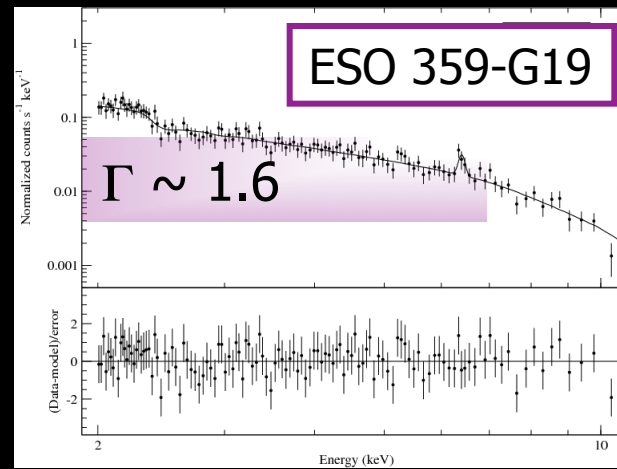
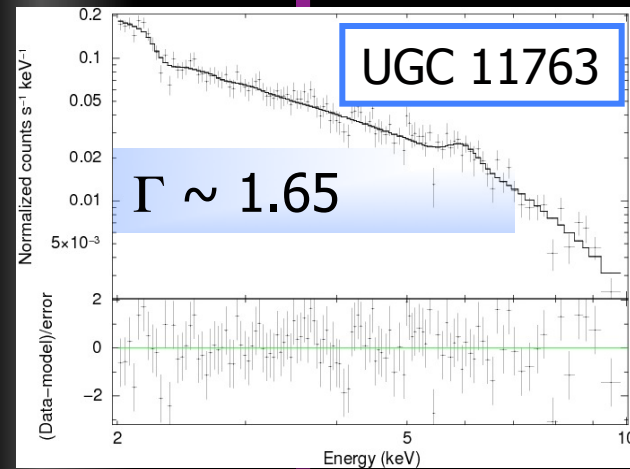
- ✧ **power law** to describe the hard X-ray spectra
- ✧ **black body/steep power law** to account for the soft excess
- ✧ **Gaussian profiles** to model the emission signatures (in the hard and soft X-ray bands)
- ✧ **a photoionization code** to characterize the absorption produced by partially ionized material whose main characteristic is a broad feature attributed to an Unresolved Transition Array (UTA) of inner-shell transitions of iron ions

PHASE (PHotoinised Absorption Spectral Engine, Krongold et al. 2003)
code parameters

- ionization parameter U : ratio between the density of ionizing photons and the density of hydrogen atoms. [$U=Q(H)/(4\pi r^2 c n_H)$]
- column density of the absorbing media (N_H)
- velocity of the material

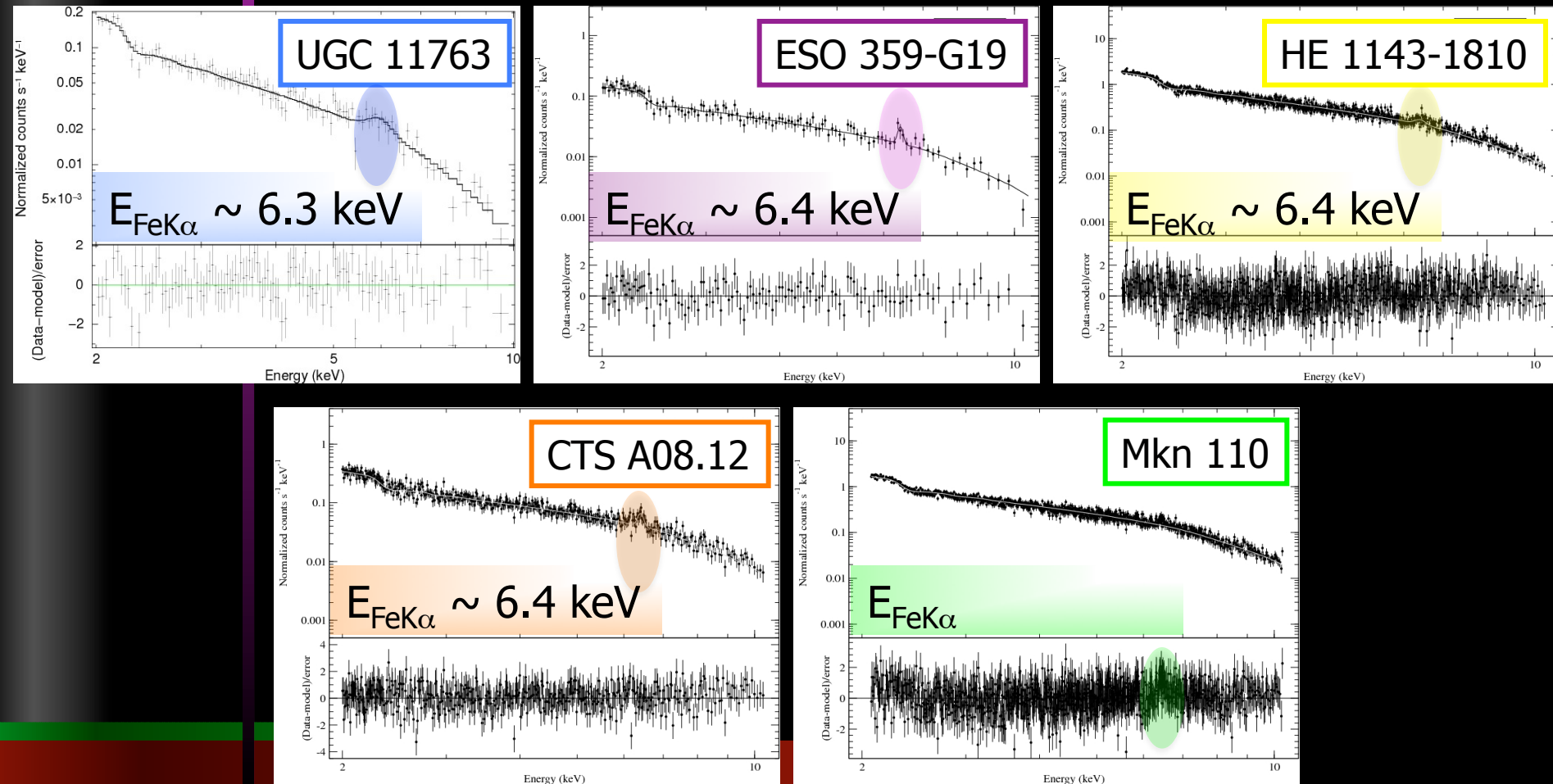
EPIIC-pn 2-10 keV fit

The continuum hard band emission of all the 5 objects is well modelled by a power law.



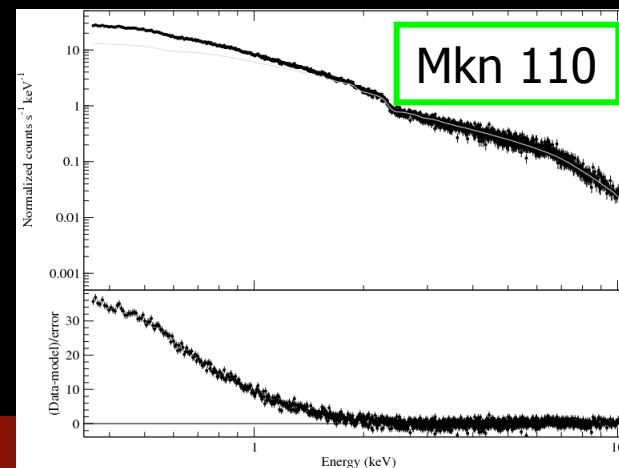
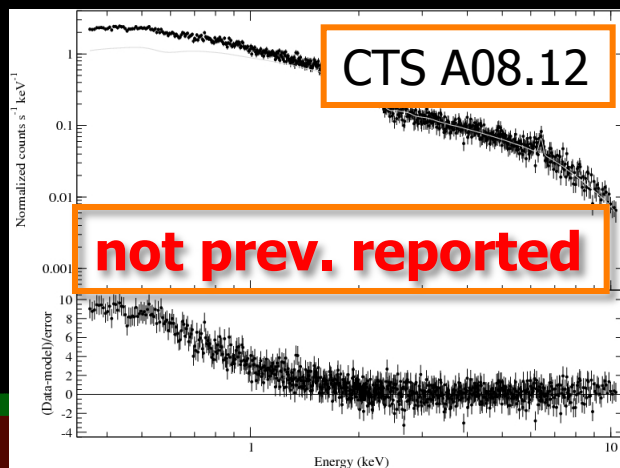
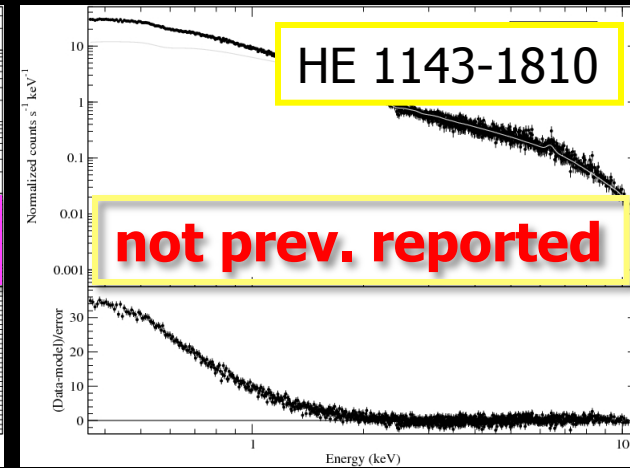
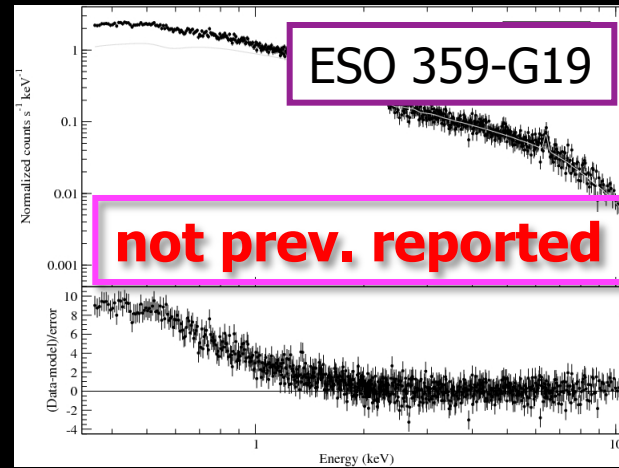
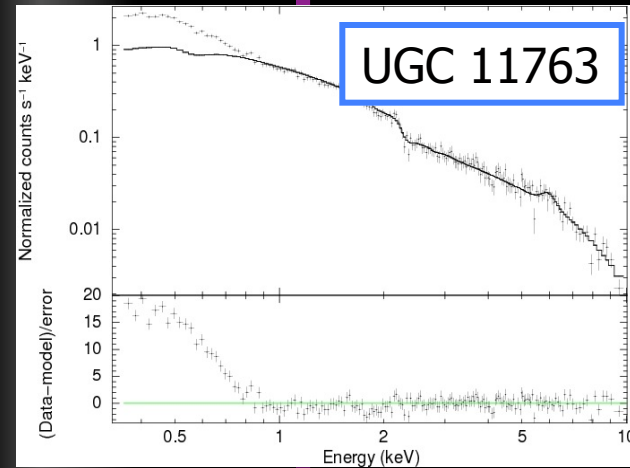
EPIIC-pn 2-10 keV fit

All the objects show signs of the presence of the neutral Fe emission line at 6.4 keV (weak and sometimes broad).



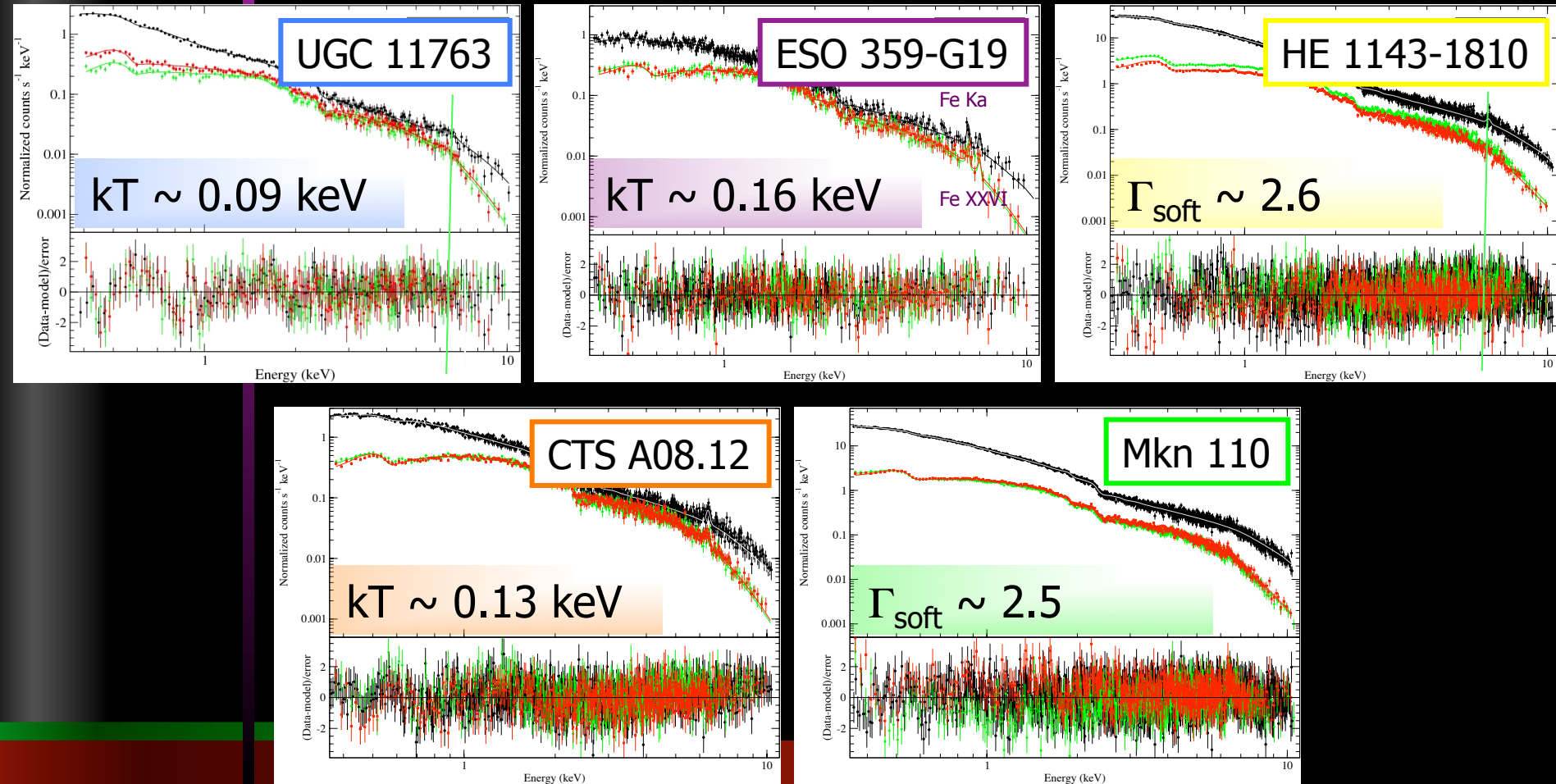
EPIc-pn 0.35-10 keV

All the 5 objects show an excess of continuum emission above the extrapolation of the hard power law to lower energies



EPIC 0.35-10 keV fit

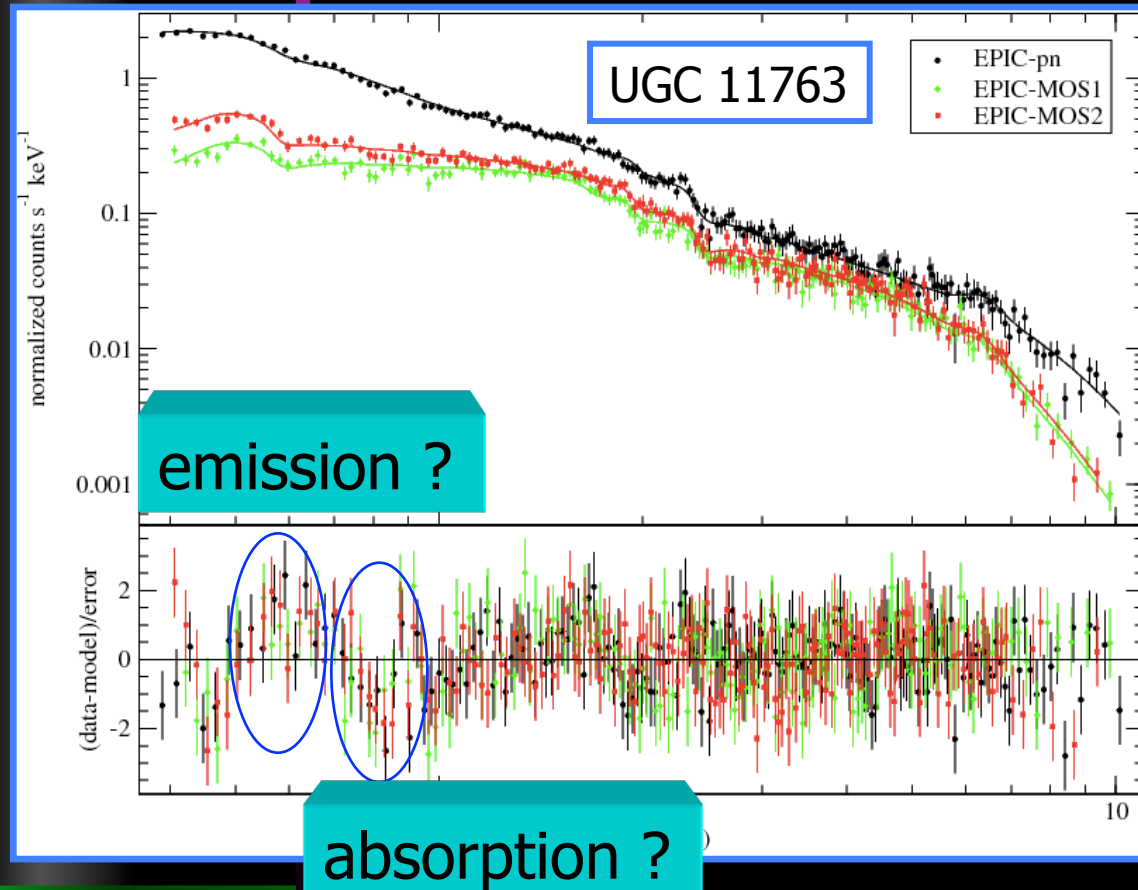
To model the soft excess we fit simultaneously the three EPIC spectra.



EPIC 0.35-10 keV fit

UGC 11763

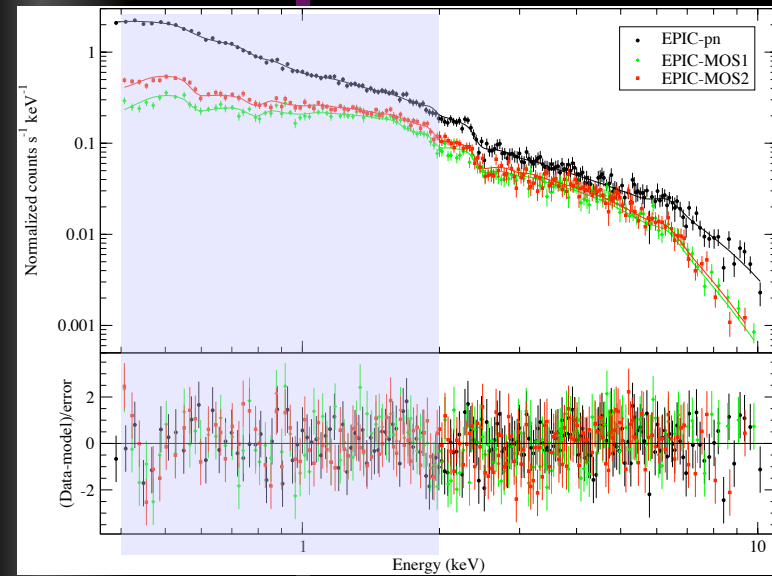
The EPIC spectra of UGC 11763 show hints of something more complex than just continuum.



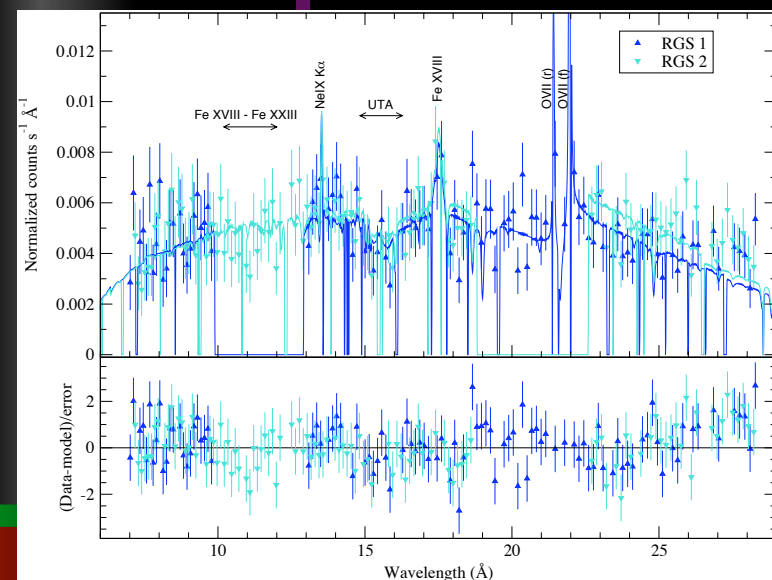
There could be absorption around 15-17 Å, that for other objects was seen as a broad absorption feature attributed (using RGS data) to an Unresolved Transition Array (UTA) of 2p-3d inner-shell absorption by iron L-shell ions (the $n=2 \rightarrow 3$ transitions)

EPIC & RGS fit

UGC 11763



	LIC	HIC
log U	1.65 (+0.07,-0.08)	2.6 (+/- 0.1)
N_H	$10^{21.2} (+/- 0.2) \text{ cm}^{-2}$	$10^{21.51} (+/- 0.01) \text{ cm}^{-2}$
vel	500 (+/- 300) km/s	500 (+/- 300) km/s
T	$1.8 (+/- 0.2) \times 10^5 \text{ K}$	$1.2 (+/- 0.1) \times 10^6 \text{ K}$



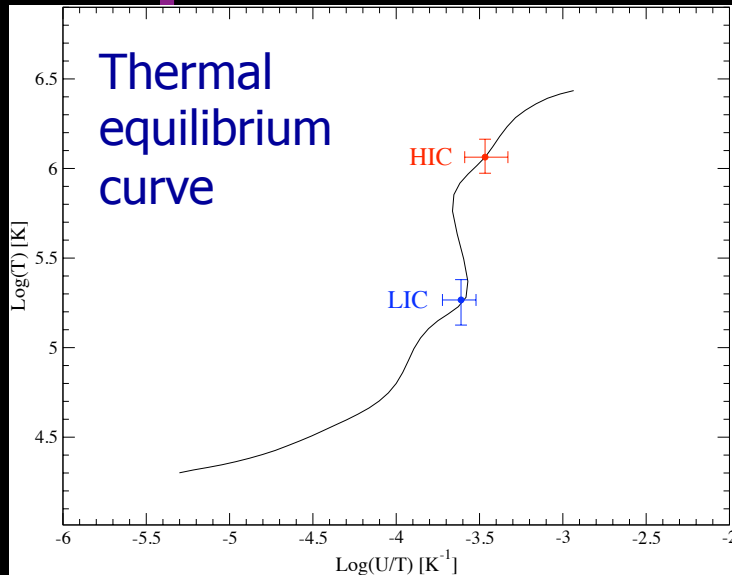
Two absorbing components are clearly required to fit the data (as seen in other objects with warm absorbers)

we find two partially ionized **absorbing components** with distinct ionization states and identical kinematics

EPIC & RGS fit

UGC 11763

Placing the absorbing components on the thermal equilibrium curve



points where heating and cooling processes are in equilibrium

$\log(U/T)$ is inversely proportional to gas pressure

vertical lines indicate isobaric conditions

LIC & HIC lie in stable parts of the curve

consistent with having the same gas pressure

+

LIC & HIC are kinematically indistinguishable

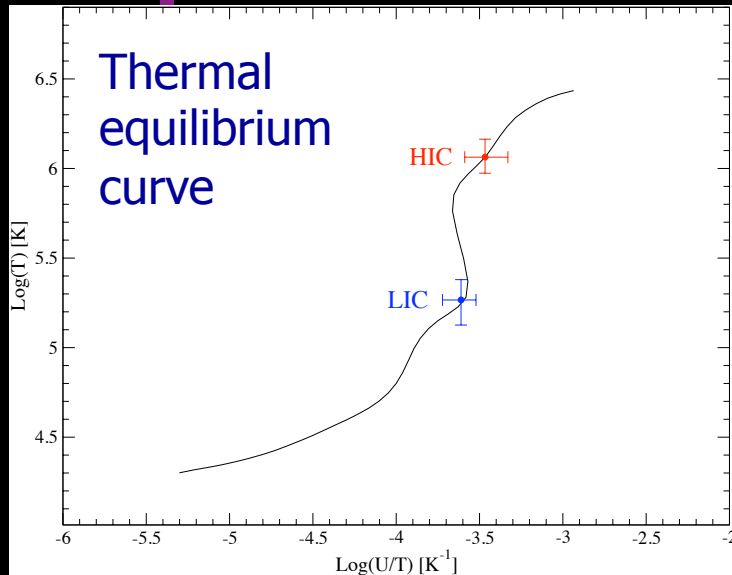
⇩

LIC & HIC could constitute two phases of the same medium

EPIC & RGS fit

UGC 11763

Comparing with what is found in other Seyfert galaxies:



LIC in other Seyfert galaxies are cooler: $T \sim \text{few } 10^4 \text{ K}$

and UTA produced by Fe VII-Fe XII

In this source LIC temperature is $T \sim 1.8 \times 10^5 \text{ K}$

First time!!!!

UTA formed by Fe XIII-Fe XV

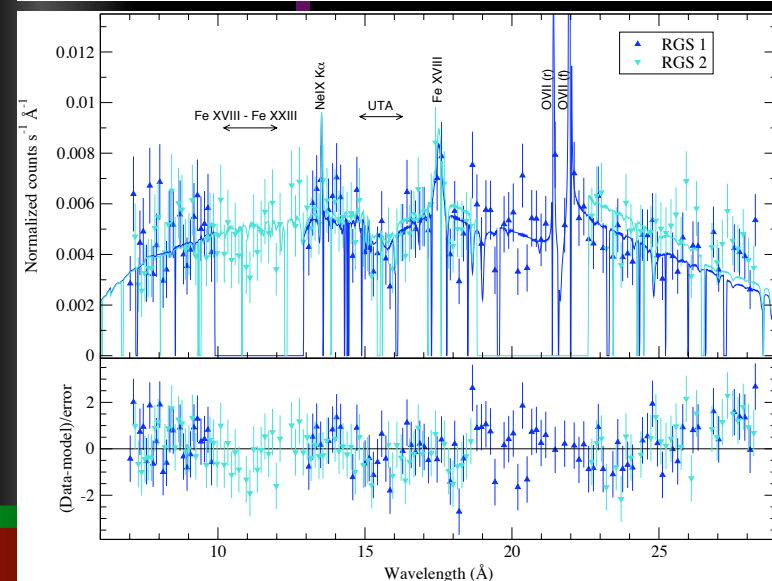
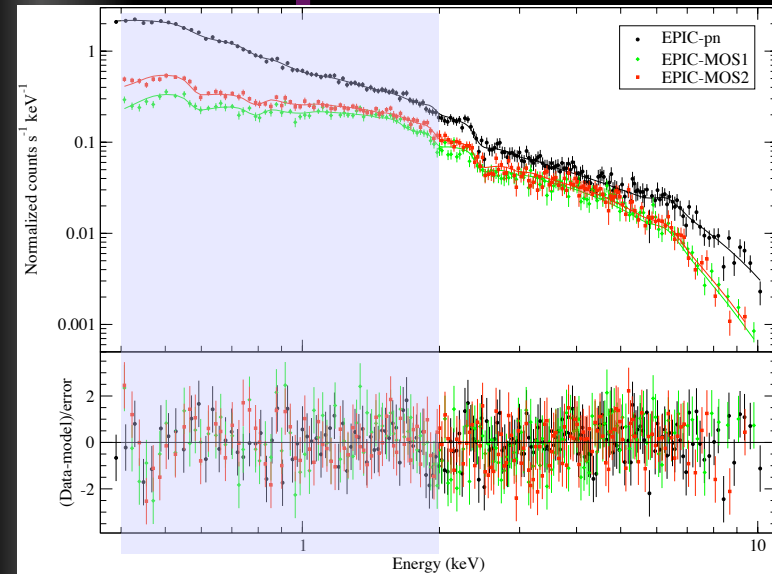
Only gas at such high temperature could coexist in pressure equilibrium with the HIC component

UGC 11763

EPIC & RGS fit

In the soft band, we find 4 statistically significant **emission lines**, even though their parameters are not completely constrained.

None of these lines are resolved in the spectra, which does not allow the reliable determination of their widths.



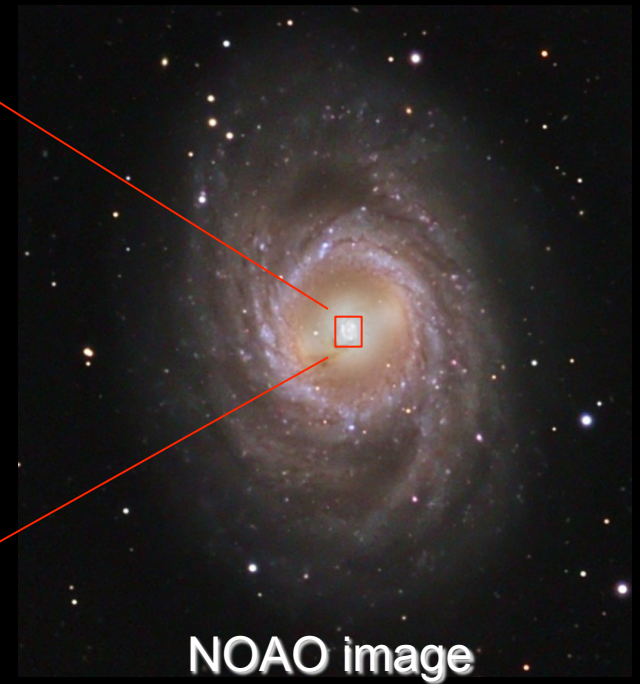
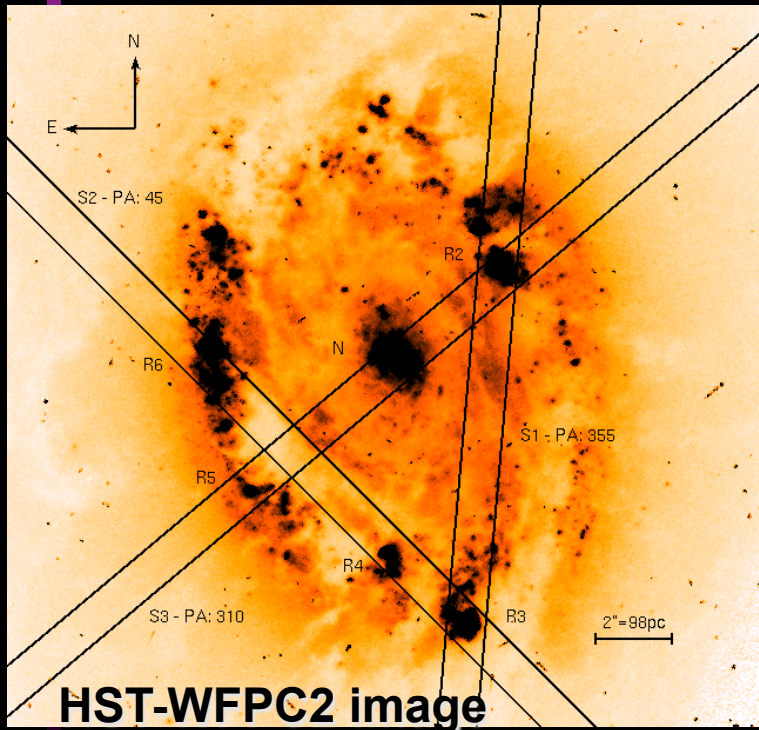
Fe K α	$E=6.4 (+0.2/-0.3) keV$
OVII (f) 22.10 Å	$\lambda = 21.97^* \text{Å}$
OVII (r) 21.60 Å	$\lambda = 21.41^* \text{Å}$
FeXVIII 17.65 Å	$\lambda = 17.50 (+0.11/-0.09) \text{Å}$
NeIX (blend)	$\lambda = 13.52 (+0.1/-0.2) \text{Å}$

Study of Circumnuclear star-forming regions using X-rays

Mónica Cardaci
&
Guillermo Hägele

CNSFRs

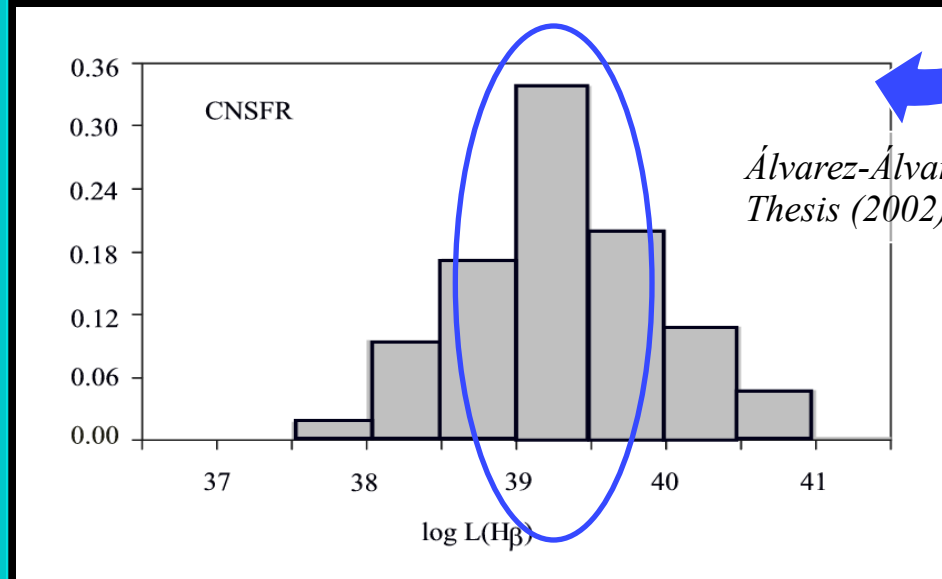
The bulges of some nearby spiral galaxies show **intense star-forming regions** located in a **roughly annular pattern** around their nuclei.



Why CNSFRs?

Their large *H α* luminosities, point to *relatively massive star clusters as their ionization source.*

They provide clues for the understanding of star formation phenomena at large metallicities, and, being close to the nuclear regions, for the determination of metallicity gradients in spiral galaxies.



What is our aim?

Using X-rays data we want to study the properties of the **“hot” phase of the ionized gas** in HII regions to obtain an independent measure of their abundances.

An oxygen abundance lower than expected from empirical abundance indicators points to a deficiency of light alpha elements (O, Ne) in the central regions.

This effect was found in M 82 (Origlia et al. 2004)

Data acquired

Long observations of about **110ks** (~ 30.5 hs) for each galaxy



NGC2903

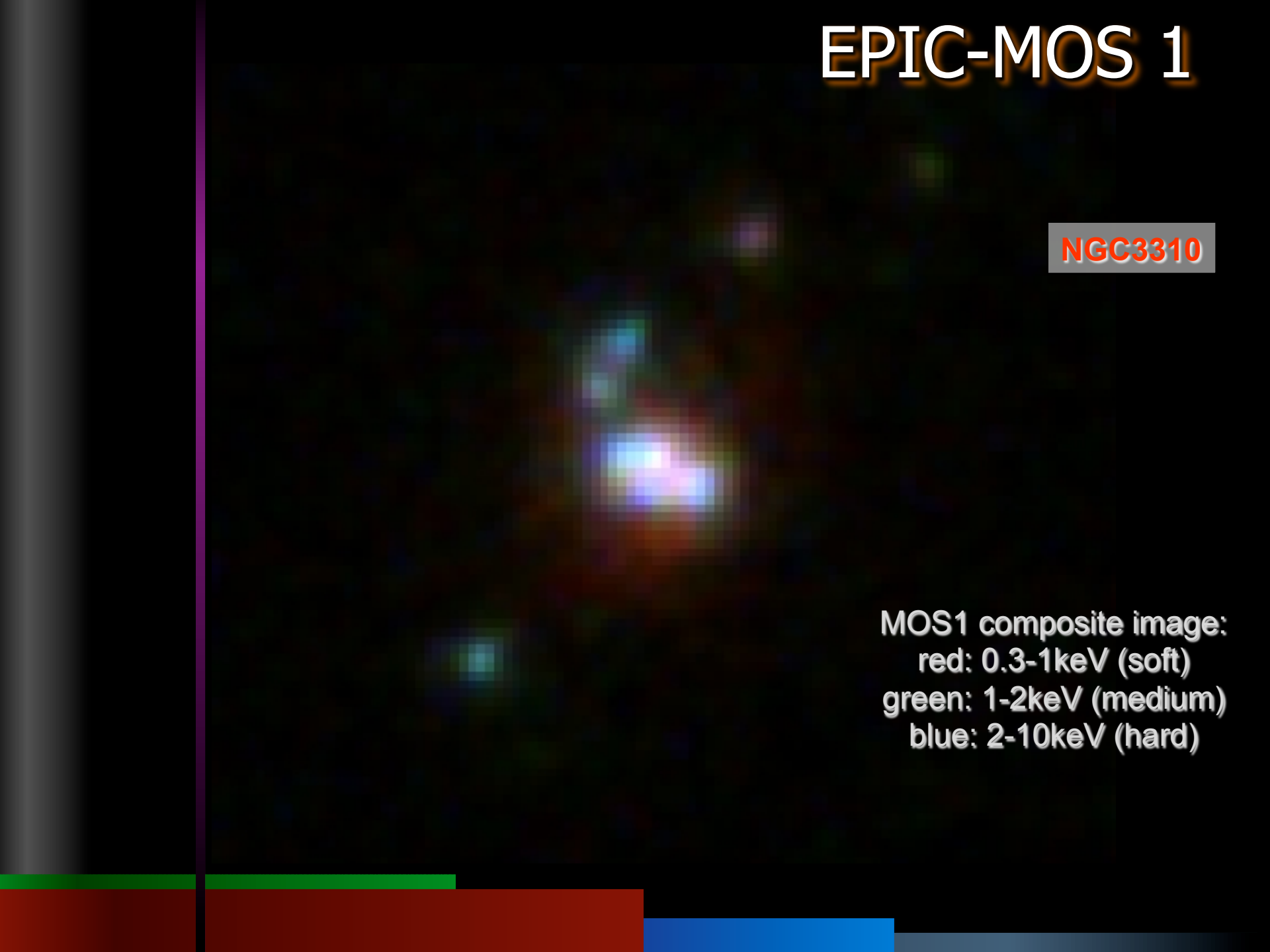


NGC3310

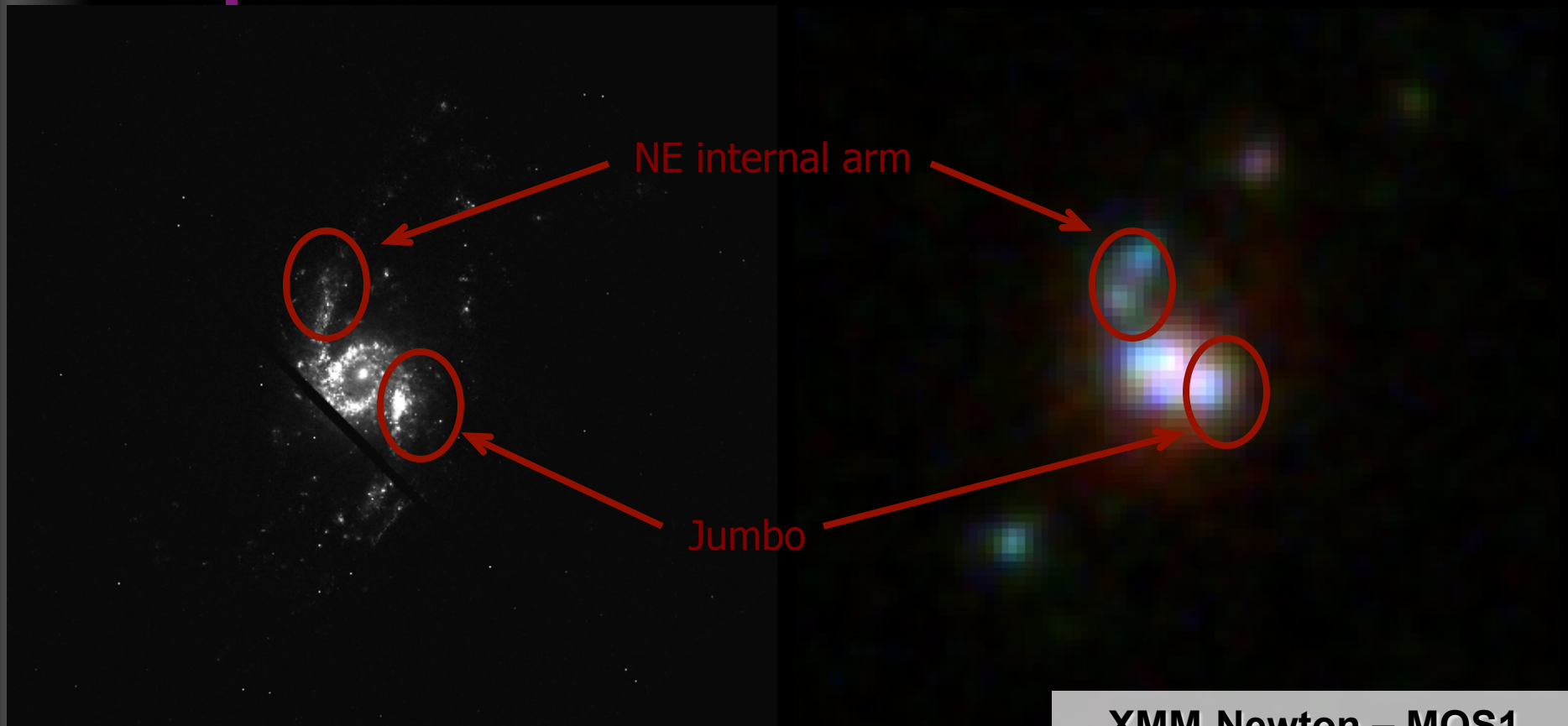
EPIC-MOS 1

NGC3310

MOS1 composite image:
red: 0.3-1keV (soft)
green: 1-2keV (medium)
blue: 2-10keV (hard)

The image shows a composite of X-ray data from the EPIC-MOS 1 instrument. The central region is dominated by a bright, multi-colored source, likely a galaxy nucleus, with a core of red and green emission and a surrounding blue halo. Several other fainter sources are visible in the field. The image is presented in a false-color format where red represents soft X-rays (0.3-1 keV), green represents medium energy X-rays (1-2 keV), and blue represents hard X-rays (2-10 keV). A vertical purple line is visible on the left side of the image, and a horizontal bar at the bottom is divided into red, green, and blue segments.

ACS & EPIC-MOS 1



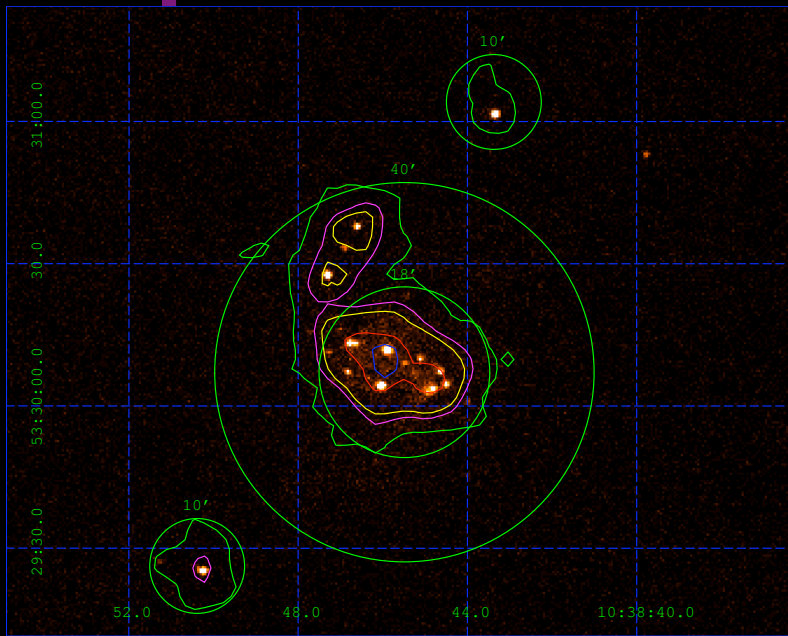
HST – ACS
F658N - H α

XMM-Newton – MOS1
red: 0.3-1keV (soft)
green: 1-2keV (medium)
blue: 2-10keV (hard)

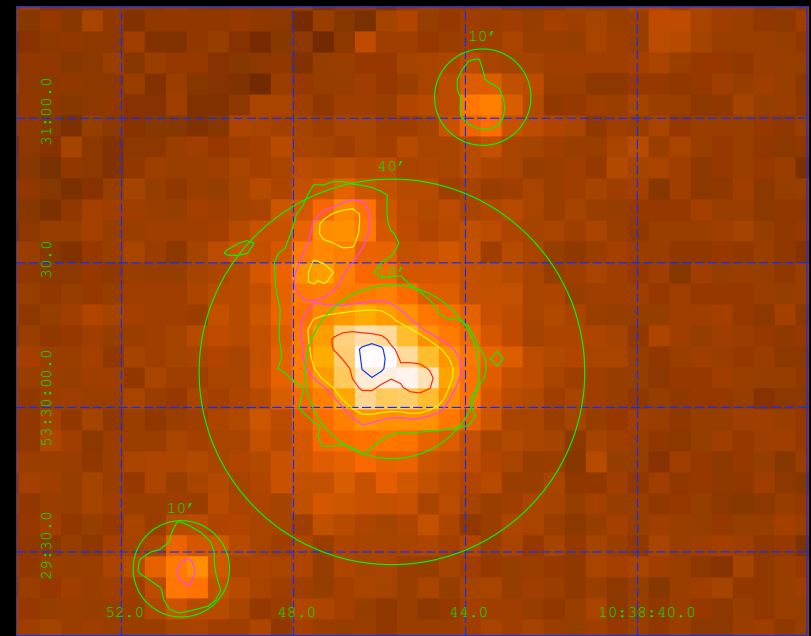
ACIS-S & EPIC-MOS 1

NGC3310 has also been observed using the ACIS-S camera on board Chandra satellite (spatial resolution of $\sim 1''$ & moderate spectral resolution). On this data it was possible to identify punctual sources and broad spectral features.

Comparing contours from our XMM-Newton EPIC-pn camera data (with a spatial resolution of $\sim 6''$) with Chandra data we can see a perfect match in the identification of the emitting regions.



Chandra – ASIS-S (2003)



XMM-Newton – EPIC-MOS1

There is only one study of this type and was performed by Origlia et al. in 2004 (in M82).

This is a new insight for the abundance determination in high metallicity environments.

Thanks